ABCM Symposium Series in Mechatronics

TOPOLOGY OPTIMIZATION APPLIED TO 2D AND 3D ELECTRICAL IMPEDANCE TOMOGRAPHY

Cícero Ribeiro de Lima
Dept. of Mechatronics and Mechanical Systems Engineering - University of São Paulo - 05508-900, Brazil
cicerorl@usp.br

Luis Augusto Motta Mello
Dept. of Mechatronics and Mechanical Systems Engineering - University of São Paulo - 05508-900, Brazil
luis.mello@poli.usp.br

Emílio Carlos Nelli Silva
Dept. of Mechatronics and Mechanical Systems Engineering - University of São Paulo - 05508-900, Brazil
ecnsilva@usp.br

Abstract. *Electrical Impedance Tomography (EIT) is an imaging technique which tries to find conductivity distribution inside a section of body. The EIT deals with an inverse problem in which given the measured voltages on electrodes it estimates the conductivity distribution by using an image reconstruction algorithm. EIT can be used in several applications and, recently, it has been applied for obtaining images in medical applications. Several types of reconstruction algorithms have been reported and used. In this work, images of lungs are obtained by applying Topology Optimization Method as reconstruction algorithm in EIT. Solution of this optimization problem is obtained combining the Finite Element Method and a sequential Linear Programming algorithm (SLP). Since it is an ill-posed problem, regularization schemes based on spatial filters and included constraints are used. The SLP allows to include easily regularization schemes and to work well even though under high noisy measurements. Reconstruction of some 2D and 3D examples using numerical and experimental data are shown.*

Keywords*: Topology Optimization, Electrical Impedance Tomography, Finite Element Method*

1. Introduction

Since the beginning of 90´s years, a technique called Electric Impedance Tomography (EIT) has been studied as an interesting alternative for obtaining images on clinical applications. In fact, EIT has been applied to geophysical sciences (Parker, 1984; Ramirez *et al*., 1993) and in non-destructive testing (Santosa, Kaup and Vogelius, 1996; Santosa and Vogelius, 1991), however in medical procedures its application is recent (Cheney, Isaacson and Newell, 1999; Borcea, 2002). EIT is based on an inverse problem where, given the voltages measured on electrodes positioned on the boundary of body, it tries to find the conductivity distribution inside of body, and as a consequence its image. A sequence of low intensity electrical currents is applied to the body section, through electrodes positioned around the patient's body and aligned in a plane corresponding to a transverse section of the body (Cheney, Isaacson and Newell, 1999), as illustrated in Figure 1.

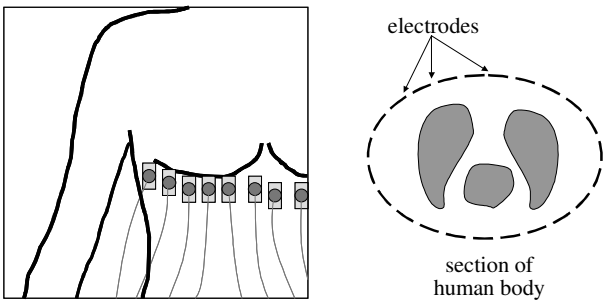

Figure 1 – Electrodes positioned around the body.

Technology of EIT is safer and cheaper than other tomography techniques and although it has poor resolution it has potential for clinical applications such as monitoring mechanical ventilation of lungs (Amato *et al*., 1998) and monitoring heart function and blood flow (Holder, 1993). Moreover an EIT device is portable which allows its installation for continuous monitoring of bedridden patients, which avoids dangerous patient transportation from ICU (Intensive Care Unit) to the exam room. In this technique the patient does not have exposition to any type of radiation, just to the low electrical current levels that do not cause any harm to the patient (Cheney, Isaacson and Newell, 1999).

This work presents results obtained from application of Topology Optimization Method (TOM) to EIT image reconstruction. TOM tries to find systematically a material distribution inside of a design domain, to extremize an objective function requirement, satisfying some specified constraints (Bendsøe and Sigmund, 2003). The topology

optimization problem applied to EIT consists on finding a material distribution (or conductivity distribution) of a body that minimizes the difference between electrical potentials obtained from electrode measurements at the boundary of the body and electrical potentials simulated numerically from a computational model of this body. This optimization problem is solved by a computational algorithm that combines Finite Element Method (FEM) with an optimizer called Sequential Linear Programming (SLP) (Haftka, Gürdal and Kamat, 1996), which allows us to include easily several constraints in optimization problem than other algorithms applied to obtain image in EIT. It is interesting because it constrains the solution space avoiding images without clinical meaning on tomography examination. Moreover, it is known that SLP provides little numerical error propagation.

The FEM mesh of domain is not changed during the optimization process. The FEM formulation is generated from constitutive equation of the conductive medium, which is given by Poisson's equation (Muray and Kagawa, 1985). Thus, electrical potential distribution in the discretized domain is obtained by the following equilibrium FEM system of equations (Bathe, 1996):

$$\mathbf{K}\,\mathbf{\Phi} = \mathbf{I} \tag{1}$$

where $\mathbf{K}$ is the global electric conductivity matrix of FEM model, $\mathbf{\Phi}$ is a nodal electric potential vector and $\mathbf{I}$ is a nodal electric current vector. In this work, the FEM model of the discretized domain uses quadrilateral elements (2D model) or tetrahedral elements (3D model) and, in addition, a FEM electrode model, proposed by Hua, *et al.* (1993), has been applied to represent the electrical behavior of the electrode-electrolyte interface layer. Figure 2 shows the electrode element that is considered in that model.

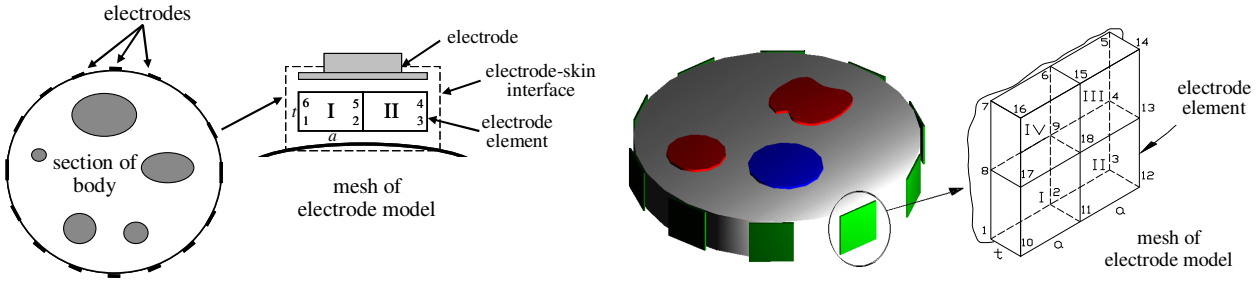

a) 2-D model b) 3-D model

Figure 2 – Electrode model.

For this electrode model, the electric potential on the surface of the metal electrode (nodes 4, 5 and 6 in 2-D model, for example) is assumed to be uniform. The electrical conductivity matrix (kel) of the electrode element depends on width of an electrode, thickness of the contact interface (electrode-electrolyte) and of resistivity value of the contact interface, as demonstrated by Hua, *et al.* (1993). The product between resistivity and thickness of the contact interface is known as contact impedance (or electrode parameter) of electrode elements. Each electrode element matrix kel is inserted in the global matrix $\mathbf{K}$ in according to its connectivity.

In TOM, the material in each point of domain (or in each element) can vary from a material "A" to another one "B" according to a material model, which allows design variables of optimization problem to go from one material to another in a continuous way. For instance, material "A" could be air and material "B" could be the tissue of lungs. In this work, the material model applied is known as Density Method (Bendsøe and Sigmund, 1999) that defines the conductivity properties ($\mathbf{c}_k$) of each element of domain in the following way:

$$\mathbf{c}_k = \rho_k{}^p \mathbf{c}_A + \left(1-\rho_k{}^p\right)\mathbf{c}_B \qquad \text{with} \qquad 0 \le \rho_k \le 1;\ k = 1...N \tag{2}$$

where $\mathbf{c}_A$ and $\mathbf{c}_B$ are the conductivity properties of base materials of the domain, p is a penalization coefficient of intermediates materials, and N is number of finite elements. The value of each design variable ρ_k is defined between 0 (presence of "B" only) and 1 (presence of "A" only).

In the next section, the formulation of topology optimization applied to EIT and its numerical implementation are presented. In section 3, image reconstruction results using numerical and experimental data are shown. Finally, in section 4, some conclusions are given.

2. Optimization Problem Formulation and Its Numerical Implementation

The image reconstruction by EIT using TOM can be interpreted as a problem of finding the material distribution inside the domain that reproduces the measured electric potential values at electrodes. Thus, the optimization problem could be:

$$\text{Minimize:} \quad F = \frac{1}{2}\sum_{j=1}^{ne}\sum_{i=1}^{np}\left(\phi_{ij} - \phi_{ij0}\right)^2 \tag{3}$$

Such that: *electrical conductivity equation*
$0 \le \rho_k \le 1 \; ; \quad k = 1...N$
and *additional constraints*

where F is the objective function in which ϕ_{ij0} and ϕ_{ij} are the measured and simulated electrical potential values, respectively. The values ϕ_{ij} are obtained by computational model of the domain. The *ne* and *np* values are the number of applied current load cases and the number of measurement points (electrodes), respectively. The optimization problem above is an ill-posed problem, which finds different distributions of conductivities in the domain that yield the same voltage values on electrodes. However, TOM allows us to include easily some constraints in the optimization problem, restricting the solution space and regularizing the problem. Thus, additional constraints could be included for improvements in problem solution.

The solution of topology optimization problem shown in Eq. (3) is obtained numerically by iterative optimization algorithm sketched in Fig. 3. The FEM model of the design domain is supplied to the algorithm as initial data. By analysis of the FEM model, the electric potentials (ϕ_{ij}) are calculated, allowing us to obtain the objective function and constraints values. In the next step, the optimization is done by using the gradients of the objective function and constraints, relative to design variables (sensitivity analysis). The optimization is done by using the gradients of the objective function and constraints relative to design variables, which are calculated analytically through an adjoint method (Cook and Young, 1985; Byun *et al*., 1999). The optimization algorithm is started with an uniform distribution of material for the whole design domain and it supplies a new material distribution (design variables), which is updated in the FEM analysis.

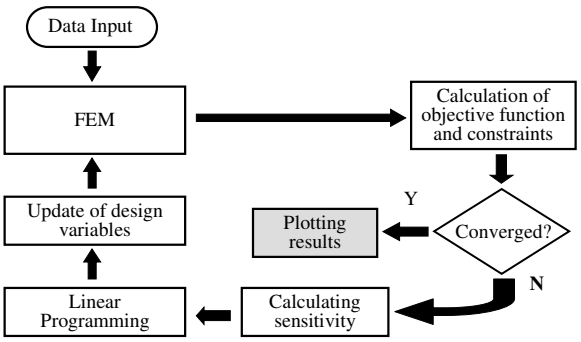

Figure 3 – Flowchart of the TOM algorithm.

The optimization algorithm above, implemented using C language, is known as Sequential Linear Programming (SLP), which has been successfully applied to topology optimization. The SLP allows us to work with a large number of design variables and complex objective functions, and solves a non-linear optimization problem considering it as a sequence of linear sub-problems, which can be solved with Linear Programming (LP) (Haftka, Gürdal and Kamat, 1996). The non-linear problem of Eq. (3) can be linearized by writing a Taylor series expansion of the objective function and keeping only the terms with first order derivatives. For that approach to be valid it is necessary to limit the variation of design variable value in each linear sub-problem by using moving limits (Haftka, Gürdal and Kamat, 1996). In each iteration of topology optimization process, the SLP finds the optimum value for the design variables, that it will be used in the subsequent iteration as initial value. Thus, this process continues successively, until the convergence for the objective function value is achieved.

3. Results

In this section, some 2D and 3D examples will be presented to illustrate image reconstruction using this software with numerical and experimental data. For all examples presented here, electric current load is considered equal to 1 milliampere, which is applied following an adjacent pattern of electrical excitation, as illustrated in Fig. 4. Moreover, in these examples, the topology optimization algorithm uses penalization coefficient value (p) equal to 2.

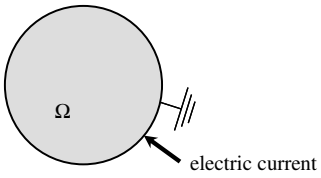

Figure 4 – Adjacent pattern of electrical excitation in EIT.

In this work, to obtain a good quality image for clinical applications in EIT, thirty two 10-mm-wide electrodes are uniformly positioned along the boundary of the design domain (Tang *et al.*, 2002). To find the electrical potentials in these electrodes a pair of them is excited electrically, following the adjacent pattern (see Fig. 4), where the potential in one of them is made to be null ("ground") and the other receives the low intensity electrical current. The pair of electrodes is successively changed until an enough number of observations under different angles is obtained and a high quality image is generated.

3.1. 2-D examples

In this section, the performance of the implemented algorithm is evaluated through 2-D examples and by using numerical and experimental phantoms. First, image of two objects in the domain is obtained by using numerical data and artificial noise. After, the algorithm is applied to obtain an image in a circular domain through using experimental data, in which noise measurements are considerable.

3.1.1. Using numerical data to obtain image of two objects in the domain

The desired image is shown in Fig. 5a, where clear and dark regions simulate a material with 1/17 $(\Omega m)^{-1}$ (clear region) and 10^{-6} $(\Omega m)^{-1}$ (dark regions). In practice, this situation would be equivalent to keep some regions with air in a saline domain, for instance. A numerical phantom, whose domain is uniformly discretized in 3072 four node quadrilateral elements (with thickness equal to 35 millimeters) is considered to simulate accurately the measured electrical potentials (ϕ_{ij0}). On the other hand, a less refined mesh (1120 elements, see Fig. 5b) is applied for image reconstruction. This reduces the computational time to calculate the value of design variables (related to the number of mesh elements) and avoids the inverse crime. The images are obtained from an elliptical domain whose larger axis is 400 millimeters.

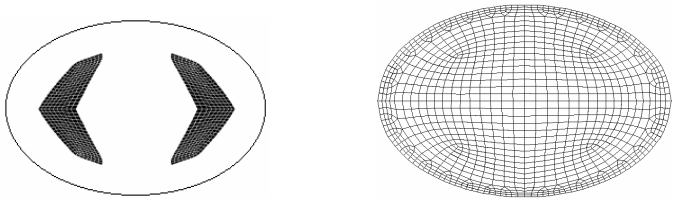

Figure 5 – a) Image to be reconstructed; b) Mesh to obtain image (1120 elements).

In this case, the electrode parameters (see section 1) must also be estimated separately from optimization process. Thus, a numerical phantom (3072 elements) containing only one material (without dark regions) and an electrode parameter value equal to 100 $(\Omega.m^2)^{-1}$ for all electrode elements are adopted to obtain the measured voltages (ϕ_{ij0}) of a saline medium. Based on these voltages values and the less refined mesh (1120 elements), and considering the electrode parameters as design variables, the topology optimization algorithm obtains the optimum electrode parameter values for any initial guess. Since two different domain discretizations are used, numerical errors due this are absorbed by optimized electrode parameters. Therefore, it is noted that most of optimized electrode parameters were not obtained necessarily close to the adopted value of the numerical phantom. In this case, most of them fell in an average error about 10% for adjacent pattern, however some of them were obtained close to 50% of the adopted value.

As mentioned before, the implemented algorithm allows us to include easily some constraint in optimization problem. Thus, in this example, a kind of image tuning could be included to improve the estimated conductivity values. This constraint is given by the following equation:

$$\sum_{k=1}^{N} V_k \rho_k \geq V^* \tag{4}$$

where V_k is the volume of each element and V^* is the material constraint inside of the domain. It is previously known that dark regions in Fig. 5a represents 18% (V^*) of total volume of elliptical domain.

Then, by using this tuning control and the optimized electrode parameters, we obtain the following images and corresponding absolute conductivity values of dark region elements.

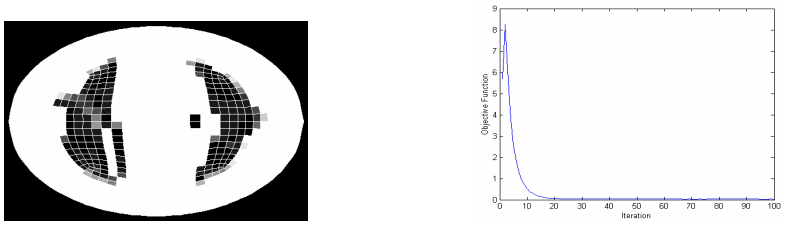

a) obtained image b) convergence curve

Figure 6 – Obtained result with tuning.

From the graph of convergence of the objective function, we observe that it drops quickly to a minimum value, however it continues iteration after iteration with a very small oscillation until the best image is found. Absolute conductivity values of elements of low conductivity (dark regions) are closer to the expected absolute value adopted in this work (10^{-6} $(\Omega m)^{-1}$). In this case, the conductivity values of dark regions have an average of about 82.4% of expected value.

Now, to verify the robustness of the algorithm to work with noise, we have introduced a random variation with standard deviation of about 15% (positive and negative) of the measured electrical potential (ϕ_{ij0}) of each electrode obtained through numerical phantom. Images in Fig. 7 show that the method can absorb this noise level (artificial) in adjacent pattern of electrical excitation.

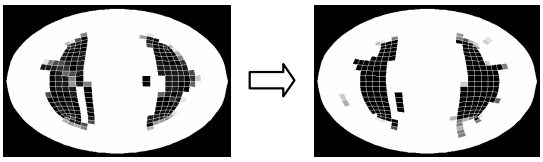

a) without noise b) with noise

Figure 7 – Results considering noise from adjacent pattern.

3.1.2. Using experimental data

Here, the software was evaluated by using data obtained from an experimental phantom. The desired image is shown in Figure 8a. In this case, the experimental phantom is a cylindrical container whose diameter is equal to 230 millimeters and it was filled up to 35 millimeters with a saline solution of concentration 0.3 gram/liter of NaCl, which conductivity value is equal to 1/17 $(\Omega m)^{-1}$. The dashed line in the phantom (see Fig. 8a) represents presence of a immersed glass object, which conductivity value is equal to 10^{-6} $(\Omega m)^{-1}$.

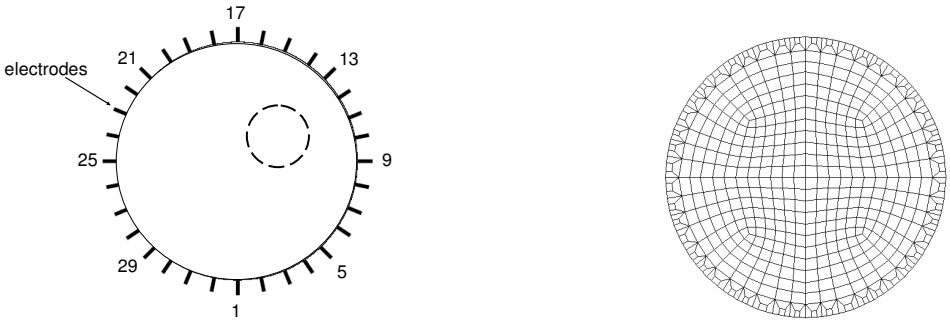

a) b)

Figure 8 – a) Image to be reconstructed; b) Mesh to obtain image (576 elements).

In this example, a "coarse" mesh with 576 four node quadrilateral elements (see Fig. 8b) is applied to image reconstruction. A two-phase method, proposed by Trigo, Lima and Amato (2004), is adopted as strategy to estimate electrode parameters and the conductivity distribution for this case. This strategy considers the problem of estimating electrode contact impedances separated from the problem of image estimation. Thus, in an alternation way of the successive runs of iterative process, first the implemented algorithm estimates the electrode parameters, considering

them as design variables in optimization process, and after that estimates conductivity distribution of the domain with the glass object.

For this example some regularization schemes, based on included constraints, are applied in optimization problem. One of them is a spatial filtering scheme based on smooth distribution of the design variables in whole domain (Swan, Kosaka and Reuss, 1997; Cardoso and Fonseca, 1999), which makes better the control of variation of the design variable values. This filter changes the move limits in the following way (Cardoso and Fonseca, 1999):

$$\rho_i = \frac{\rho_i V_i + \overline{w}\sum_{j=1}^{nv}\rho_j V_j}{V_i + \overline{w}\sum_{j=1}^{nv} V_j} \qquad \text{with} \quad \overline{w} = \frac{\sum_{k=1}^{nv} w_k}{nv} \;;\; w_k = \frac{R_{\max} - R_{ij}}{R_{\max}} \tag{5}$$

where *Vi* is the volume of element *i*, *nv* is the number of adjacent elements *j* adopted around of the element *i*, *Rij* is the distance between centers of element *i* and *j* and *Rmax* is a radius that accomplishes all adjacent elements *j*. Here, the image is obtained considering a *Rmax* value that accomplishes at least a number of eight elements *j* around of a central element *i*.

The other regularization scheme is a constraint based on weighted distance interpolation, which is given by following equation:

$$\sum_{k=1}^{N}\frac{1}{d_k^2}\rho_k \geq \sum_{k=1}^{N}\frac{1}{d_k^2}\overline{\rho}_k \tag{6}$$

where $\overline{\rho}$ is average conductivity of the domain and d_k is the distance measured from center of each element up to center of the domain. This constraint makes the balance of conductivity values of each element in the domain. The average conductivity is a parameter of optimization process that can be obtained by considering the domain as a resistor, whose resistance value can be calculated through Ohm's law.

Thus, next figures show the obtained image and its corresponding convergence curve obtained by using the adjacent pattern of electrical excitation.

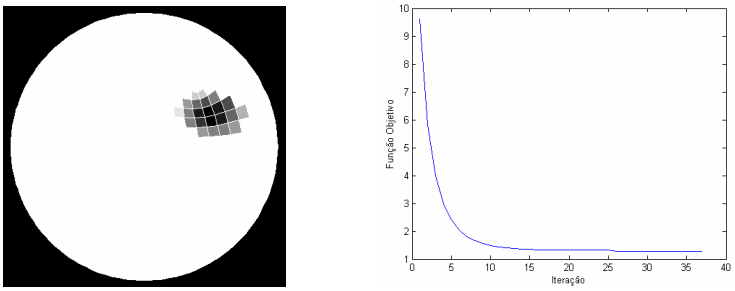

a) obtained image b) convergence curve

Figure 9 – Obtained result with spatial filter and weighted distance interpolation scheme.

According to the obtained image (see Fig. 9a) we note that implemented algorithm is able to detect the glass object inside of phantom. Following the convergence of objective function (see graph of Fig. 9b), we observe that it fells quickly to a minimum value in 20 iterations approximately. However, absolute conductivity values of most elements in dark region (that represents the glass object) have an average of about 70% of expected value.

3.2. 3-D examples

In the 3-D example only numerical data is used to evaluate the implemented algorithm to obtain image. As an alternative to the material model previously presented (and applied in 2-D reconstruction), the algorithm is implemented based on the CAMD (Continuous Approximation of Material Distribution) approach where fictitious densities are interpolated in each finite element, providing a continuum material distribution in the domain (Matsui and Terada, 2004). In CAMD, nodal design variables are introduced, and the material model becomes:

$$\mathbf{c}_k = \left(\sum_{m=1}^{nd} H_m \rho_m\right)^p \mathbf{c}_A + \left[1 - \left(\sum_{m=1}^{nd} H_m \rho_m\right)^p\right]\mathbf{c}_B \qquad \text{with} \qquad 0 \leq \rho_m \leq 1 \tag{7}$$

where ρ_m is the m^{th} nodal design variable, H_m is a FEM shape function (Bathe, 1996) and *nd* is the number of nodes per element.

The central section of desired image is shown in numerical phantom of Fig. 10b, where clear and dark regions simulate a material with high conductivity (1/17 $(\Omega m)^{-1}$) and low conductivity (10^{-6} $(\Omega m)^{-1}$), respectively. In this case, images are obtained from a cylindrical domain of radius 220 millimeters and 35 millimeters high, and the conductivity distribution is uniform along the axis of the domain.

A numerical phantom whose domain is discretized into 34359 four node tetrahedral elements (see Fig. 10a) is analyzed through FEM and each electrical potential ϕ_{ij0} is obtained. The image reconstruction is then carried out in a less refined mesh with 5548 tetrahedral elements (see Fig. 10c).

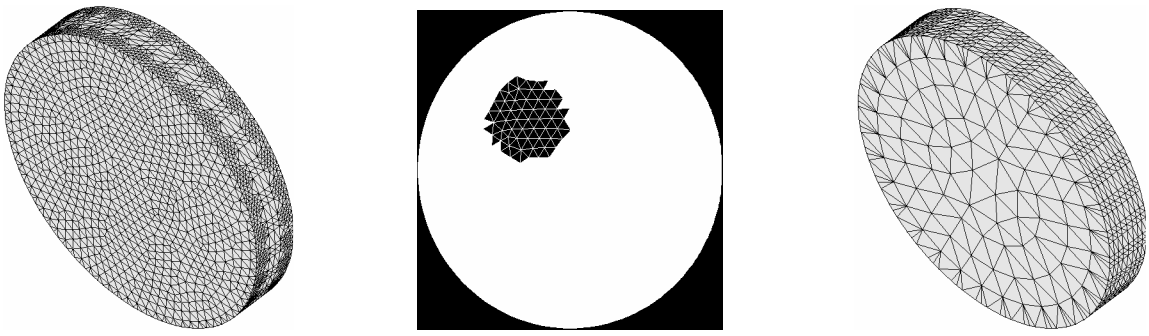

a) numerical phantom b) central section of the phantom c) mesh to obtain image

Figure 10 – a) Numerical phantom (34359 elements) to obtain potentials ϕ_{ij0}; b) The central section of phantom and image to be reconstructed; c) A less refined mesh (5548 elements) applied to obtain the image.

Here, electrode parameters (see section 2) must also be obtained based on numerical data in an analogous way made for 2-D example (see section 3.1.1). Using these optimized electrode parameters, applying the spatial filter and a constraint similar to the constraint based on weighted distance interpolation (shown in section 3.1.2), and considering the same level of artificial noise described in section 3.1.1, the following image is obtained (see Fig. 11a). For simplicity, only the central section is presented (like the phantom, the result is piece-wise uniform along the axis of the domain).

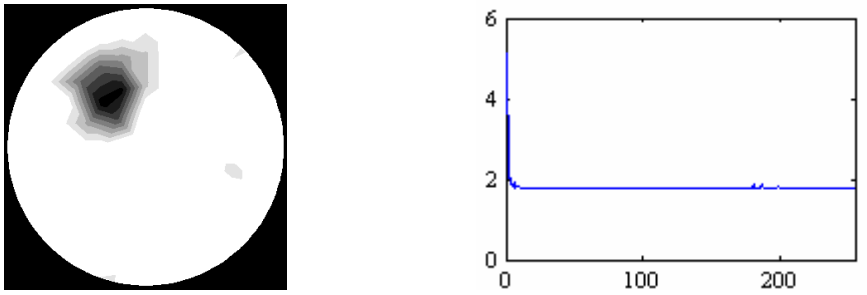

a) obtained image b) convergence curve

Figure 11 – 3-D obtained results with CAMD.

According to the results, the algorithm reduces spatial variation of obtained conductivity distribution. It is mainly attributed to the fact that there is a significant difference between the number of design variables and the amount of information (electrical potentials) available. Following the convergence of objective function (see Fig. 11b), we observe that it fells quickly to a minimum value (1.77). Besides, absolute conductivity values in dark region of the domain have an average of about 45% of expected value.

4. Conclusion

A computational algorithm of Topology Optimization Method (TOM) applied to obtain image in Electrical Impedance Tomography (EIT) was proposed. This algorithm was implemented in software written in C language. According to our results, it is noted that by using numerical and experimental data the software is able to obtain, in few iterations and with a certain level of precision, the contact impedance values of interface electrodes-skin and the values of absolute conductivity of two materials inside of the domain and consequently the image desired, even if noise is introduced. As a future work, other regularization schemes based on included constraints in topology optimization will be tested to improve the precision in obtaining absolute conductivity values.

The implemented algorithm of TOM could be seized for obtaining images of lungs through an EIT device. The TOM allows us to include easily some constraints in the problem of image reconstruction limiting the solution space during tomography examination and avoiding images without clinical meaning. Moreover, it becomes easier to limit the design domain where presence of air in the lung can occur and, therefore, allows us to work with known areas inside of the domain (bone, heart, etc).

5. Acknowledgements

The first and second authors would like to acknowledge the financial support of FAPESP (Fundação de Amparo à Pesquisa do Estado de São Paulo), through a doctoral (nr. 02/01625-0) and a master (nr. 02/10574-0) scholarship. All authors also thank the national research support CAPES (Coordenação de Aperfeiçoamento de Pessoal de Nível Superior).

6. References

Parker, R. L.,1984, "The Inverse Problem of Resistivity Sounding", Geophysics, Vol.142, pp. 2143-2158.

Ramirez, A. *et al*.,1993, "Monitoring an Underground Steam Injection Process Using Electrical Resistance Tomography", Water Resources Res., Vol.29, pp. 73-87.

Santosa, F., Kaup, P. and Vogelius, M.,1996, "A Method for Imaging Corrosion Damage in Thin Plates from Electrostatic Data", Inverse Problems, Vol.12, pp. 279-293.

Santosa, F. and Vogelius, M.,1991, "A Computational Algorithm For Determining Cracks From Electrostatic Boundary Measurements", International Journal Eng. Sci., Vol.29, pp. 917-938.

Cheney, M., Isaacson, D. and Newell, J.C.,1999, "Electrical Impedance Tomography", SIAM review, Vol.41, No. 1, pp. 85-101.

Borcea, A. L.,2002, "Electrical Impedance Tomography", Inverse Problems, Vol.18, pp. 99-136.

Amato, M. B. P. *et al*.,1998, "Effect of a Protective-Ventilation Strategy on Mortality in the Acute Respiratory Distress Syndrome", Journal of Medicine, New England, 338, pp. 347-354.

Holder , D.,1993, "Clinical and Physiological Applications of Electrical Impedance Tomography", UCL, Press, London.

Bendsøe, M. P. and Sigmund, O.,2003, "Topology Optimization: Theory, Methods and Applications", Springer-Verlag, New York.

Haftka, R. T, Gürdal, Z. and Kamat, M. P.,1996, "Element of Structural Optimization", Kluwer Academic Publishers, Boston.

Muray, T. and Kagawa, Y.,1985, "Electrical Impedance Computed Tomography Based on a Finite Elements Model", IEEE Trans. on Biomed. Eng., Vol.32, pp. 177-184.

Bathe, K. J.,1996, "Finite Elements Procedures", Prentice Hall, New Jersey.

Hua, P. *et al*.,1993, "Finite Element Modelling of Electrode-Skin Contact Impedance in Electrical Impedance Tomography", IEEE Trans. on Biomed. Eng., Vol.40, pp. 335-343.

Bendsøe, M. P. and Sigmund, O.,1999, "Material Interpolations Schemes in Topology Optimization", Archive of Applied Mechanics, Vol.69, pp. 635-654.

Cook, R. D. and Young, W. C.,1985, "Advanced Mechanics of Materials", Macmillan, New York.

Byun, J. K. *et al*.,1999, "Inverse Problem Application of Topology Optimization Method with Mutual Energy Concept and Design Sensitivity", Proceed. of IEEE Magnetic, pp. 296-300.

Tang, M. *et al*.,2002, "The Number of Electrodes and Basis Functions in EIT Image Reconstruction", Inst. of Physics Publishing, Physiol. Meas., Vol.23, pp. 129-140.

Trigo, F.C., Lima, R.G. and Amato, M. B. P.,2004, "Electrical Impedance Tomography Using the Extended Kalman Filter", IEEE Transactions on Biomedical Engineering, Vol.51, pp.72-81.

Swan, C., Kosaka, I. and Reuss, V.,1997, "Topology Optimization for Structures with Linear Elastic Material Behaviour", International Journal of Numerical Methos in Engineering, Vol.40, No.1, pp. 3033-3057.

Cardoso, E. L. and Fonseca, J. S. O.,1999, "Intermediate Density Reduction and Complexity Control in the Topology Optimization", Anais do Cobem'99, Águas de Lindóia.

Matsui, K. and Terada, K.,2004, "Continuous Approximation Of Material Distribution for Topology Optimization", International Journal for Numerical Methods In Engineering, Vol.59, No. 14, pp. 1925-1944.

7. Responsibility notice

The authors are the only responsible for the printed material included in this paper.